CUME EXAM # 367

This exam is worth 75 points. It is based on the accompanying paper by Sánchez-Lavega et al. (2010), "The impact of a large object on Jupiter in 2009 July" Astrophys. J. Let. 715, L155-L159, plus ancillary materials related to this topic provided from other papers. A grade of 70% or higher is expected to be a passing grade. You may use a calculator, but only for algebraic and trigonometric types of calculations – you may NOT use a calculator to store formulae, constants, etc.

Things You Might Need to Know

1 AU = 1.496×10^{13} cm Jupiter's equatorial radius = 71,492 km Jupiter's oblateness = 0.065Jupiter's rotational period = $9^h55^m27.3^s$ Jupiter's orbital semimajor axis = 5.20 AU $G = 6.674 \times 10^{-8}$ dyn cm² g⁻²

Observations

- 1. The paper states that the images in methane absorptions show the impact spot to be brighter than its surrounding, suggesting that the material was high in the atmosphere. Explain why a bright debris plume would indicate a high altitude at these wavelengths. (3 points)
- 2. Panel B in the attached set of images from Figure 2 of Orton et al. (2011) shows an image of the plume in an H_2 filter at 2.12 μm . Yet in astrophysics, we often use CO as a proxy for H_2 in galaxies and the ISM.
 - a) How is it that we can observe H_2 in Jupiter's atmosphere but not in the ISM? In other words, what makes CO a good proxy for H_2 in the ISM, and why is H_2 not detectable in astrophysical environments but detectable on Jupiter? (3 points)
 - b) The H₂ transition at 2.122 μ m is the v=1-0, J=3-1 S(1) line. What does each of those terms mean? (3 points)
 - c) Contrast your answer in part (b) with a methane absorption band, e.g. at 0.889 μ m. [An image of Jupiter at 0.889 μ m is shown in the attached Figure 1 of Hammel et al. (2010).] What kind of transition(s) give rise to the 0.889 μ m methane absorption band? How is this kind of transition(s) different from a CO line observed at 115 GHz? (4 points)



- 3. The impact was said to be located at a planetocentric latitude of 55.1°. What is the definition of a planetocentric latitude, as opposed to a planetographic latitude, which is also sometimes used when referring to the giant planets? (2 points)
- 4. From examining the images of the impact shown in Figure 1 of the paper, estimate the seeing that Anthony Wesley must have had from his observing site in Australia in order to obtain those images. Calculate the diffraction limit of his telescope and compare your two numbers, commenting on how the images in Figure 1 could have been obtained. (10 points)

D

368,34

031 12

Giant Planet Atmospheres

- 5. Draw a Jovian pressure-temperature profile, labeling the axes and the different layers in the atmosphere. Indicate on your P-T profile where the top of Jupiter's uppermost cloud deck lies, as well as the location of the impact debris (HINT: this information can be found in the paper). (10 points)
- 6. Figure 3c from Hammel et al. (2010) shows the altitude range of the impact debris. As stated in the figure caption, this information was derived from the data shown in Figure 3b and using the thermal wind equation, which relates the vertical variation of geostrophic winds (winds that are balanced by the Coriolis and pressure gradient forces) to horizontal temperature gradients. Calculate the Rossby number for the winds in the vicinity of the impact site to determine whether in fact the geostrophic approximation holds. (10 points)

Impacts

- 7. Write a simplified version of Equation 1 for a ballistic trajectory, ignoring the Coriolis force and the sliding of falling material as it enters the atmosphere. Compute the horizontal displacement of material given the best-fit values in the paper for the ejecta parameters and compare it to the observed size of the impact streak shown in Figure 2c of the paper. Comment on the difference between the two values and how much of an effect you think the inclusion of the Coriolis effect and sliding had on the final result. (10 points)
- 8. Contrast the physics of this impact into Jupiter's atmosphere with the physics of an asteroid impact on the Earth. In your answer, <u>briefly</u> discuss the various stages of impact events and describe the differences between the two scenarios. (10 points)

Orbital Mechanics

9. a) The paper discusses the Tisserand parameter, which is a dynamical property that is roughly conserved during an encounter between a planet and a small body; its functional form is as follows:

$$T_J = \frac{a_J}{a} + 2\left[(1 - e^2) \frac{a}{a_J} \right]^{1/2} \cos(i) \tag{1}$$

where a_J is Jupiter's orbital semimajor axis, and a, e, and i are the orbital semimajor axis, eccentricity, and orbital inclination of the small body. The paper mentions Hilda asteroids as a possible source for the impactor that hit Jupiter. The Hildas are a dynamical group of asteroids in a 3:2 mean motion resonance with Jupiter; they have moderate eccentricities and inclinations. Compute T_J for a Hilda asteroid using this information and the above equation. State all of your assumptions. (8 points)

b) Based on the data plotted in Figure 4 of the paper, when must this impactor have been captured by Jupiter in order to definitely have been a Jupiter family comet (as opposed to a Hilda asteroid)? (2 points)

r= all-e2)

e-o-circle

THE IMPACT OF A LARGE OBJECT ON JUPITER IN 2009 JULY

. Sánchez-Lavega^{1,12}, A. Wesley², G. Orton³, R. Hueso¹, S. Perez-Hoyos¹, L. N. Fletcher⁴, P. Yanamandra-Fisher³, .. Legarreta⁵, I. de Pater⁶, H. Hammel⁷, A. Simon-Miller⁸, J. M. Gomez-Forrellad⁹, J. L. Ortiz¹⁰, E. García-Melendo⁹,

R. C. PUETTER¹¹, AND P. CHODAS³

Dpto. Física Aplicada I, Escuela Superior de Ingenieros, Universidad del País Vasco, Alameda Urquijo s/n, 48013 Bilbao, Spain; agustin.sanchez@ehu.es

Acquerra Pty. Ltd., 82 Merryville Drive, Murrumbateman, NSW 2582, Australia ³ Jet Propulsion Laboratory, California Institute of Technology, 4800 Oak Grove Drive Pasadena, California, 91109, USA Atmospheric, Oceanic and Planetary Physics, Clarendon Laboratory, Parks Road, Oxford OX1 3PU, UK

⁵ Escuela Universitaria Ingeniería Técnica Industrial, Plaza de la Casilla 3, 48012 Bilbao, Spain ⁶ University of California, 601 Campbell Hall, Berkeley CA 94720, USA ⁷ Space Science Institute, 4750 Walnut Avenue, Suite 205, Boulder, CO 80301, USA ⁸ NASA Goddard Space Flight Center, Greenbelt, MD 20771, USA ⁹ Fundació Observatori Esteve Duran, Montseny 46 - Urb. El Montanya, 08553 Seva, Barcelona, Spain ¹⁰ Instituto de Astrofísica de Andalucía, CSIC, Apt. 3004, 18080 Granada, Spain

11 Center for Astrophysics and Space Science, 9500 Gilman Drive, La Jolla, CA 92093, USA Received 2010 January 19; accepted 2010 April 28; published 2010 May 12

ABSTRACT

On 2009 July 19, we observed a single, large impact on Jupiter at a planetocentric latitude of 55°S. This and the Shoemaker-Levy 9 (SL9) impacts on Jupiter in 1994 are the only planetary-scale impacts ever observed. The 2009 impact had an entry trajectory in the opposite direction and with a lower incidence angle than that of SL9. Comparison of the initial aerosol cloud debris properties, spanning 4800 km east-west and 2500 km north-south, with those produced by the SL9 fragments and dynamical calculations of pre-impact orbit indicates that the impactor was most probably an icy body with a size of 0.5-1 km. The collision rate of events of this magnitude may be five to ten times more frequent than previously thought. The search for unpredicted impacts, such as the current one, could be best performed in 890 nm and K (2.03-2.36 μ m) filters in strong gaseous absorption, where the high-altitude aerosols are more reflective than Jupiter's primary clouds.

Key words: planets and satellites: atmospheres - planets and satellites: general - planets and satellites: individual (Jupiter)

Online-only material: color figures

1. INTRODUCTION

Major impacts have modified the structure of solar system bodies (de Pater & Lissauer 2010, Chapter 5) and changed the course of biological evolution on Earth (Kasting & Catling 2003). With 70% of the total mass of the planets, Jupiter is the major attractor for impacting bodies, and its massive atmosphere constitutes a natural laboratory for studying the impact response. In 1994, several fragments of comet Shoemaker-Levy 9 (SL9) impacted Jupiter between July 16 and 22 (Hammel et al. 1995; Harrington et al. 2004). The next such an event was predicted to be hundreds of years in the future (Harrington et al. 2004). However, 15 years later a second large impact occurred. We have analyzed the impact debris in the discovery images to retrieve the impactor size, trajectory, and impact time, constraining its preimpact orbit and possible origin. We revise previous predictions on the impact rates with Jupiter and propose future search methods for their detection.

2. DEBRIS OBSERVATIONS AND ANALYSIS

The dark impact "bruise" was first noticed on CCD images of Jupiter obtained by Wesley on 2009 July 19 at 14:02 UT, just rotating into view from Jupiter's west limb (Figure 1). This feature, recorded by several amateur observers, was tracked during the next Jupiter rotation (July 20, \sim 01-02 UT) on images sent to the International Outer Planet Watch (IOPW) database. 13 The first images in methane and hydrogen absorption between

¹² Author to whom any correspondence should be addressed.

13 http://www.pvol.ehu.es/

2.12 and $2.3~\mu m$ wavelengths were obtained at NASA's Infrared Telescope Facility during the third rotation after the impact (July 20, \sim 10-13 UT) (Figures 2(a) and (b)). They showed the spot to be very bright compared to the surroundings, indicating that the material was high in the atmosphere at $\bar{P}_{\rm top} \sim 1\text{--}10~{\rm mbar}$ (Hammel et al. 2010; Orton et al. 2010), i.e., above the main Jovian clouds ($P_{\rm top} \sim 500$ mbar). However, in visible light, the feature appeared dark against the main clouds. Because its visible and near-infrared morphology and reflectivity were very similar to the previous SL9 impact observations (Hammel et al. 1995; Harrington et al. 2004), the feature was most likely formed by the debris left by an impact.

A survey of amateur observations of Jupiter obtained between \sim 0.35 and 1 μm before the identification of the debris impact (see IOPW database) indicates that the spot was not present on July 19 as late as 7:40 UT, suggesting that the impact occurred between 7:40 and 14:02 UT. Similarity with young impact debris from SL9 (Figure 2) suggests that the most probable impact time was 9-11 UT. The impact itself was not observed because it occurred on Jupiter's far side. IOPW images between June and September did not show any similar features at the same latitude bigger than \sim 200 km. We conclude that a single object impacted Jupiter on July 19, unlike the cometary fragments of

The center of the dark spot at continuum visible wavelengths was located at System-III longitude 304°.5 \pm 0°.5 and planetocentric latitude 55°.1 \pm 0°.5S, \sim 11°-12°S of the SL9 impacts (Hammel et al. 1995). The initial feature consisted of two elements: a streak (the main spot) and a low-contrast extended crescent west of the main spot (Figure 2(a)), both dark in the

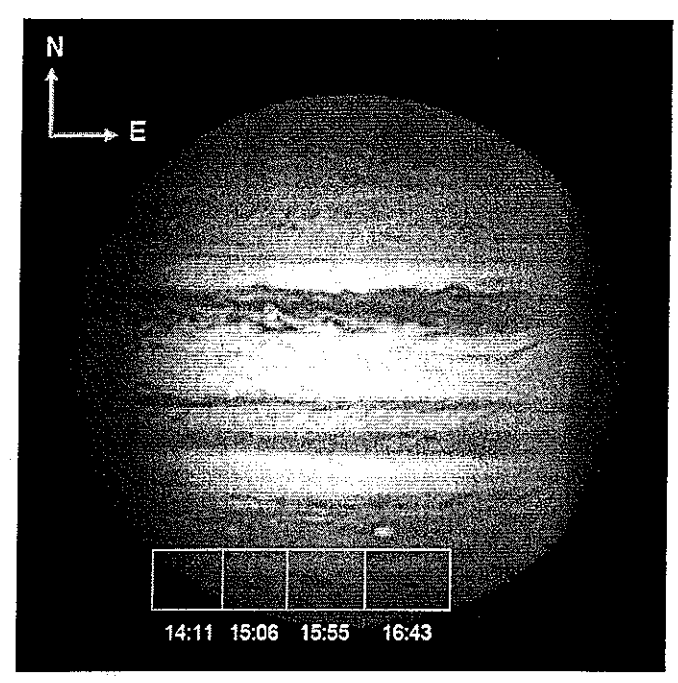


Figure 1. Discovery series of the impact debris obtained on 2009 July 19 at the indicated times (Newtonian telescope with a 368 mm diameter and a camera with a red-green-blue filter covering the spectral ranges 400-700 nm). Ninox software was used for cropping and presorting of the individual frames (Wesley 2009), with RegiStax software used for alignment and stacking (RegiStax 5 2009)

(A color version of this figure is available in the online journal.)

visible and bright in the near infrared. This is similar to what was observed for SL9, but how these features were generated by the impact is still a disputed issue (Crawford 1996; Mac Low 1996; Zahnle 1996; Takata & Ahrens 1997; Harrington & Deming 2001).

The streak had an elongated, approximately elliptical shape, with size along the major and minor axes of 6.77 in longitude (4800 \pm 200 km east—west) and 2° in latitude 2500 \pm 200 km north—south). This streak is tilted by 12° \pm 2° in the northwest—southeast direction (Figure 2(a)) relative to the latitude circle passing through its geometric center. This angle marks the approximate impactor entry direction with azimuth angle 290° (north is 0°, east is 90°, and so forth), as measured in orthographic projection (grid in km, Figure 2(c)). This is nearly opposite to the direction of the SL9 fragments, whose azimuths were all 164°.

The thin debris crescent northwest of the main spot extends 4800 km from the western edge of the streak (8800 km from its center). It is oriented with an azimuth 310° measured in the orthographic projection. Just as for the SL9 impacts (Pankine & Ingersoll 1999; Jessup et al. 2000), we interpret the 20° azimuthal clockwise rotation of the crescent, relative to the major axis of the streak, due to the action of the Coriolis force on the falling material plus a sliding in the atmosphere that conserves the tangential velocity. To check this interpretation, we present a simple model that constitutes a reasonable approach to the impact structure. At present, the available data, worse than those for the SL9, preclude a more sophisticated analysis.

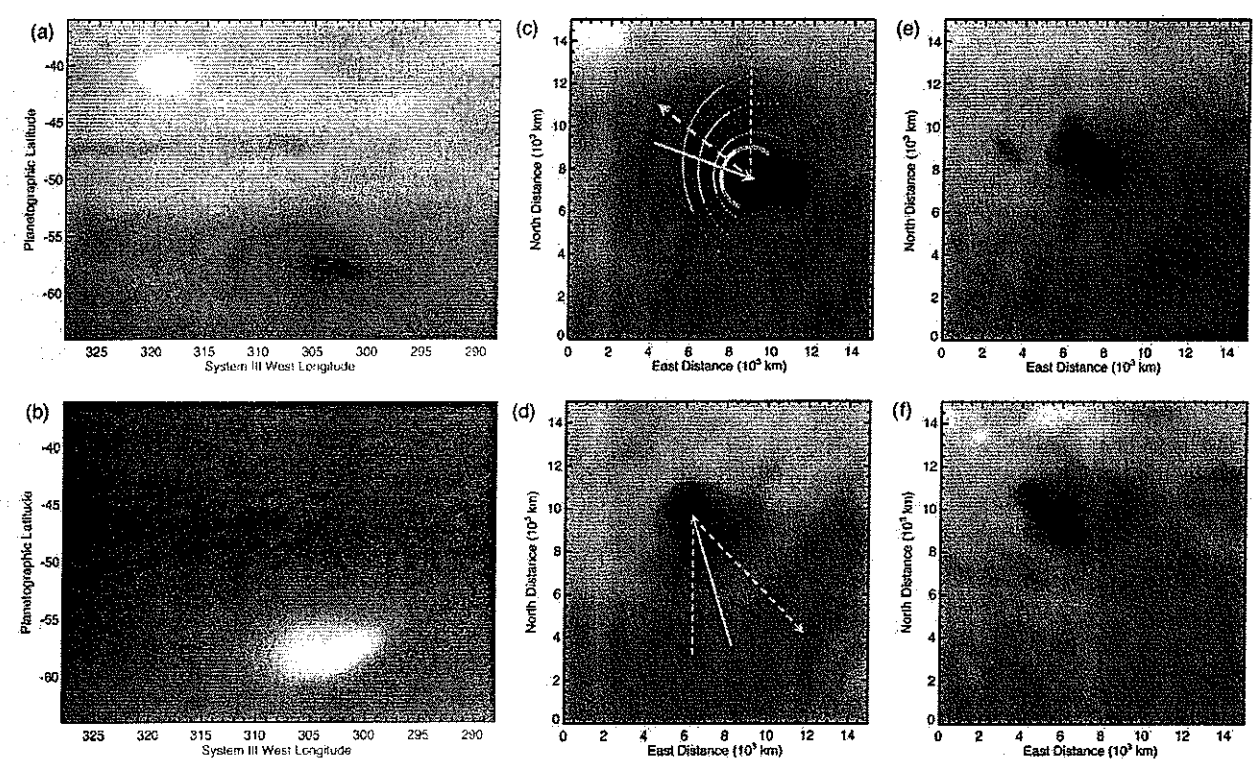


Figure 2. Map projections of Jupiter impact debris and comparison with SL9. Cylindrical maps: (a) visible wavelengths (July 19, 16:43 UT) processed with the reconstruction algorithm PIXON (Puetter & Yahil 1999). (b) near-infrared at 2.16 μ m in strong methane and molecular hydrogen absorption (July 20, 11:09 UT). The feature appears smeared northeast to southwest because of the seeing conditions. Orthographic projections (c, d, e, f): (c) 2009 July 19 impact site (as in (a)); for comparison: (d) the SL9 fragment E 2 hr after the impact. The continuous white arrows indicate the direction of the bolide entry, and the dashed arrows indicate the axis of symmetry of the plume ejecta. The arc curves are from the ballistic model of the ejecta with the thick arcs marking the horizontal range limits for times of 100 s, 300 s, and 500 s. To assess the impact time, compare frames (e) and (f) for two similar SL9 cases that correspond to impacts R after 4 hr and Q1 after 13 hr, respectively.

(A color version of this figure is available in the online journal.)

The ballistic trajectories of the ejecta are given according to Jessup et al. (2000) by

$$x(t) = \frac{1}{3}\omega g t^{3} \cos \lambda - \omega t^{2} (v_{0z} \cos \lambda - v_{0y} \sin \lambda) + v_{0x} t + x_{0}$$
(1)

$$y(t) = -\omega t^2 v_{0x} \sin \lambda + v_{0y} t + y_0$$
 (2)

$$z(t) = -\frac{1}{2}gt^2 + \omega v_{0x}t^2 \cos \lambda + v_{0z}t + z_0.$$
 (3)

Here, x_0 and y_0 mark the impact location in Cartesian coordinates, z_0 represents the 100 mb altitude level, x and y are the coordinates taken east and north from the origin at time t (see Figure 2(c)), and z is the altitude above the $z_0 = 100$ mb level. The initial-velocity components in this reference frame are (v_{0x}, v_{0y}, v_{0z}) and ω is Jupiter's angular rotation velocity. For simplicity, we assumed a constant planetocentric latitude $\lambda = 55^{\circ}$ S and constant Jovian gravitational acceleration g =25.902 m s⁻². We computed ballistic trajectories that ascend and descend over a 1600 km horizontal distance, equal to the quasi-circular left boundary of the streak (Figure 2(c)). Larger or smaller horizontal distances did not reproduce the final ejecta pattern. The horizontal distance provides a relation between the initial ejecta velocity v_0 and the elevation angle of the ejecta θ (measured from the vertical) given by $v_{0z} = v_0 \cos \theta$, with $v_0 x$ and v_0y also depending on the azimuth of the outgoing trajectory. In the ballistic trajectory, the particles modify their velocity by the action of Coriolis forces. After falling back, we assume the ejecta bounces horizontally with only horizontal Coriolis forces. The equations of motions are modified to

$$x(t) = x_f + v_{fx}t + \omega t^2 v_{fy} \sin \lambda \tag{4}$$

$$y(t) = y_f + v_{fy}t - \omega t^2 v_{fx} \cos \lambda, \qquad (5)$$

where x_f and y_f denote the horizontal point where the particle enters the 100 mbar level, and v_{fx} and v_{fy} their horizontal reentry velocity. A scale analysis of the friction of the sliding particles with the atmosphere results in sliding times of 300–500 s, consistent with those calculated for the SL9 ejecta (Pankine & Ingersoll 1999). Reentry angles $\theta < 73^{\circ}$ are discarded because (1) they would require too much time for the horizontal spread to reach the outer limits of the ejecta pattern and (2) the Coriolis deflection to the left is too high. Shallow impacts with $\theta > 75^{\circ}$ fall back too early, with no time to deflect the horizontal components of motions by the Coriolis force during the free-falling stage. The modeled crescent structure is best fitted for a ballistic trajectory of the particulates with an ejecting velocity of 7.6 \pm 0.5 km s⁻¹, an elevation angle $\theta = 70^{\circ} \pm 5^{\circ}$ (relative to the vertical), a time aloft of 195 s (horizontal range 1400 km) plus a sliding time of 400-500 s.

3. OBJECT TRAJECTORY AND ORBIT

The size of the streak's minor axis is comparable to those of Class 2a–2b SL9 impacts, but elongated in the zonal direction by a factor of 2 (e.g., fragment E is Class 2a and H, Q1, and R are Class 2b, Figures 2(d)–(f)). This could be due to a higher impact elevation angle, θ . Assuming that the zonal length of the streak was proportional to the size of the entering body and to sec θ (Mac Low 1996; Zahnle 1996), a comparison with SL9 impacts where $\theta \sim 45^{\circ}$ gives an elevation angle $\theta \sim 69^{\circ}$,

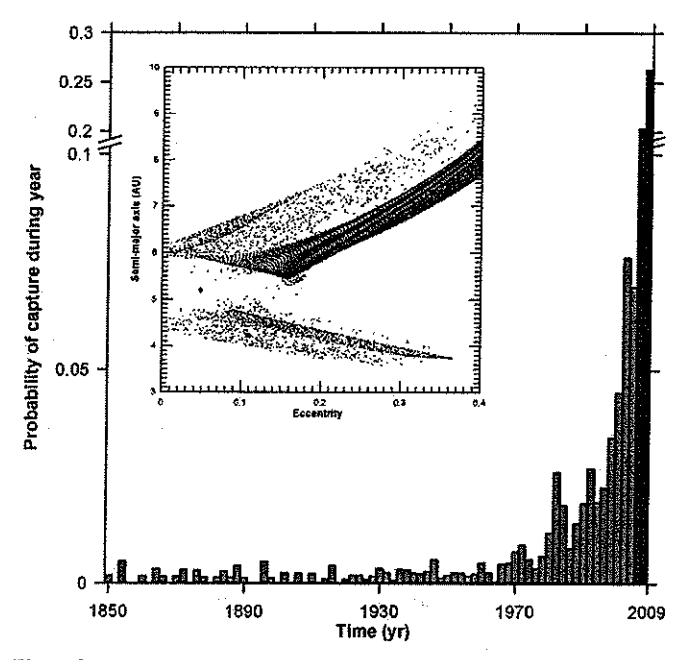


Figure 3. Histogram showing the probability that the 2009 July impact occurred directly from the object heliocentric orbit or was captured in any given year since 1850. The inset shows the scatter plot of possible heliocentric orbits (semimajor axis vs. eccentricity) for the impacting object computed from a backward integration of the derived trajectory.

(A color version of this figure is available in the online journal.)

consistent with the above crescent orientation calculations. The shallower incidence angle relative to the "horizon" indicates that the body suffered initially higher ablation per unit descent altitude, and thus might have a smaller penetration level than the SL9 impacts. Assuming the impactor was an icy body entering at Jupiter's \sim 60 km s⁻¹ escape velocity, theoretical impact models (Crawford 1996; Mac Low 1996; Zahnle 1996; Korycansky et al. 2006) of SL9 fragments with similar debris structure and albedo imply an \sim 0.5 km diameter. However, if the atmospheric ablation of the initial body size depends on the elevation angle as \sim sec θ (Crawford 1996), the pre-entry body could have been as large as \sim 1 km.

We ran backward numerical integrations of the orbital motion of the impacting body to constrain its nature and origin following the same procedure as Chodas & Yeomans (1996). A Monte Carlo analysis of more than 112,000 runs was performed, starting the integrations from an impact time window of 9-11 UT (in steps of 2 minutes) on 2009 July 19, with pre-impact velocities ranging from 54.52 to 55.1 km s⁻¹ (in steps of 0.001 km s⁻¹) relative to Jupiter's inertial reference frame. Just as for SL9, the heliocentric orbits of the candidate impactors fell into two groups: one inside and one outside of Jupiter's orbit (semimajor axis of 5.20 AU, eccentricity of 0.048, marked with a diamond in Figure 3). The integrations stopped in 1850 when motions became chaotic (Chodas & Yeomans 1996). The probability is 47% probability that this object impacted Jupiter directly from its heliocentric orbit (cases with impacts in the last 4 years) versus 53% that it was captured in Jovicentric orbit before impact, most probably after 1989. This differs from SL9, which was definitively captured before impact (Chodas & Yeomans 1996). To classify the orbit, we computed the invariant Tisserand parameter with respect to Jupiter for these runs (Figure 4). Values less than 3 indicate cometary-type orbits and values greater than 3 indicate asteroidal-type orbits. Our analysis indicates that the chance is more or less equal for the

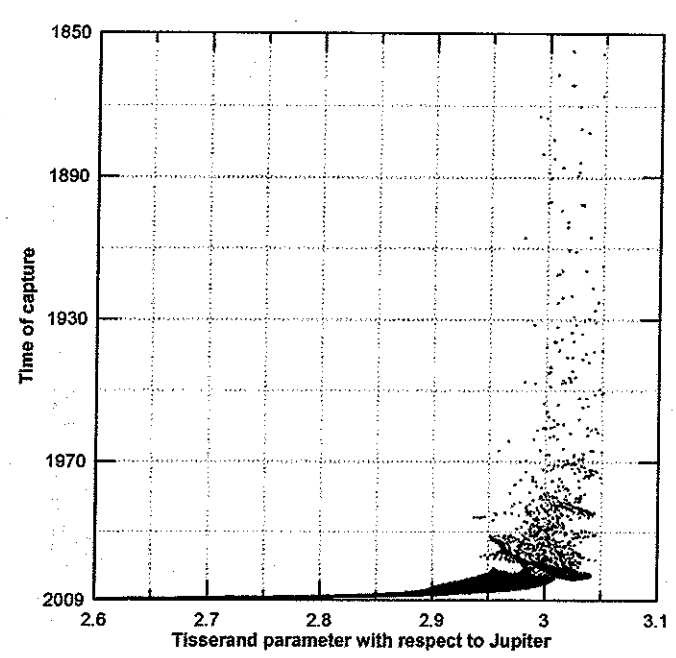


Figure 4. Scatter plot of the time needed for the impact object to reach a distance of 2 AU from Jupiter vs. the Tisserand parameter with respect to Jupiter. Beyond 2 AU, it is assumed that the orbital elements of the body are not significantly modified by Jupiter.

origin of this object to be in the main belt (Hilda asteroids or quasi-Hilda comet population) or from the Jupiter family comet population. We note that the SL9 pre-capture orbit was most probably of asteroidal type (Chodas & Yeomans 1996), belonging to the quasi-Hilda family of comets.

4. IMPACT RATES AT JUPITER AND FUTURE DETECTIONS

The impact rate of 0.5-1 km size bodies with Jupiter has been estimated to be 1 per 50-350 years (Figure 5), based on a possible impact observed by Cassini in 1690 (Schenk & Zahnle 2007), the SL9 impacts in 1994 (Hammel et al. 1995; Harrington et al. 2004), the impact crater records on the Galilean satellites (Zahnle et al. 2003; Schenk et al. 2004), and from theoretical calculations (Nakamura & Yoshikawa 1995; Kary & Dones 1996; Roulston & Ahrens 1997; Levison et al. 2000).

The 2009 event effectively doubles the available statistical sample of well-documented collisions with Jupiter. On the sole basis of SL9 and this impact, the collision rate with Jupiter for 0.5–1 km objects is 1 per 15 years. However, accounting for the ~4 month period of bad or impossible Jupiter visibility around solar conjunction and the typical ~2–3 month survival time of the scars for their identification in the visible (depending on the impact intensity, latitude, and atmospheric wind shears), the rate could be reduced to 1 impact per decade, 5–10 times the most recent impact rate calculations as shown in Figure 5.

To test this, we calculated the detection probability of the debris left by an impact with a size >0.5 km based on the available data base with observations of the planet at visible wavelengths between 1996 and 2009 (IOPW, Hubble Space Telescope 1996–2009, Cassini flyby in 2000, and New Horizons flyby in 2007). The detection probability is assumed to be unity for all high resolution imaging for a month before the observing dates, which is a characteristic time for the reconnaissance of the debris left by a 0.5 km object. For the other cases, the detection

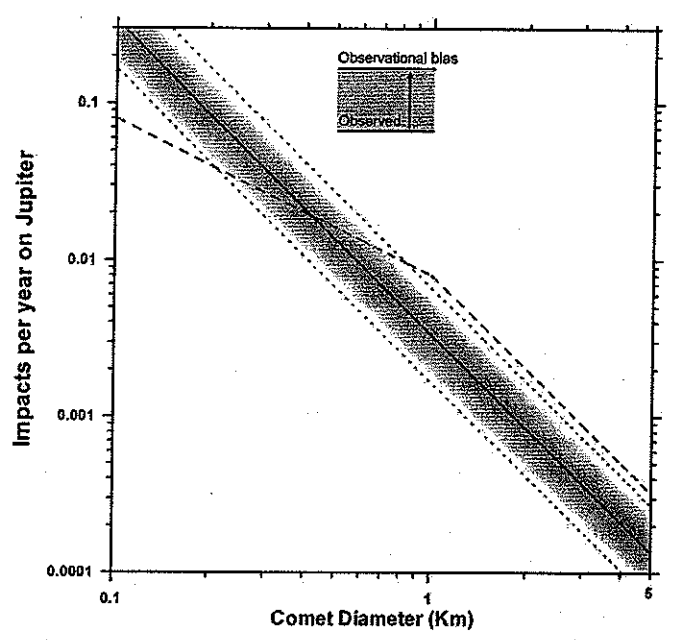


Figure 5. Cumulative impact rates per year at Jupiter as a function of the impacting object size compared to the two most recent impacts (SL9 and 2009, upper blue box). The blue dashed line is obtained with data taken from Schenk et al. (2004). The red continuous line corresponds to the scenario presented by Levison et al. (2000). The uncertainty is represented by the red dotted line boundaries obtained by multiplying the mean impact rates by 2 and 0.5.

(A color version of this figure is available in the online journal.)

probability is assumed to follow a non-normalized Gaussian distribution centered in each apparition at Jupiter's opposition and with null probability values at Jupiter's conjunctions. The FWHM of the Gaussian is assumed to follow the distribution of IOPW image contributions, amounting to more than 7000 images from 2000/2001 to 2009. For campaigns before 2001, the FWHM is assumed to be 60 days as in the following years. The maximum detection probability for IOPW data is 0.35 (35% before 2001) and 0.50 (50% after 2001) accounting for the increasing number of quality observations. We find that the integrated probability of having detected an event like this from 1996 to 2009 is $40\% \pm 6\%$, equivalent to an effective impact observing time of 5.6 \pm 0.8 years. The errors are calculated by increasing the IOPW effective probability up to 100% and decreasing the Cassini and New Horizons observing windows to include only the highest-resolution images. It should be noted that this is an upper limit, since high-resolution images are not likely to detect a small impact, especially at near-polar latitudes. In addition, the temporal variation of Jupiter's declination, which makes the relevant set of amateur observers shift from the more populous northern terrestrial hemisphere to the southern one, is not taken into account.

Additionally, we performed a Monte Carlo exploration of the probability of having an impact of a body of size larger than 500 m in Jupiter in the last 15 years based on the impact rates appearing in Figure 5 (Levison et al. 2000; Schenk & Zahnle 2007). We find a value of 8%–32%, which transforms into a 3%–13% probability of observing such an impact when taking into account the effective observing time of Jupiter in the last 15 years.

Determining the statistics and probability of impacts of large bodies with Jupiter requires a continuous imaging survey. In the CCD imaging range (continuum wavelengths from 350 nm to 1 μ m), the impact debris is darker than Jovian clouds, and

could be identified to a size as small as ~300 km. The current large number of amateurs using CCD webcam imaging and stacking processing methods allows for a survey in much greater depth (in time and resolution on the planet) than 10 years ago, when less efficient single CCD imaging was employed, or 20 years ago when photography and visual drawing was performed by a smaller number of amateurs (Rogers 1995). This was probably why previous events were not detected. The discovery and identification of unpredicted impacts, such as the current one, could be best performed in the near-infrared methane absorption bands at 890 nm for optical CCDs and even better in near-infrared methane-hydrogen absorptions with the K band (2.12–2.3 μ m), where the high-altitude aerosols make the impact features much brighter than Jupiter's primary clouds. Optimal results would be obtained by dedicated telescopes, imaging Jupiter regularly in these wavelengths, complemented by deep imaging surveys near Jupiter searching for impact bodies to allow planning and preparation for observing impacts itself, as occurred with SL9.

This work was supported by the Spanish MEC AYA2006-07735 and MICHN AYA2009-10701 with FEDER and Grupos Gobierno Vasco IT-464-07. G.O. and P.Y.F. acknowledge support from NASA grants to JPL. L.N.F. was supported by NASA Postdoctoral Program at the Jet Propulsion Laboratory (Caltech, USA). J.L.O. acknowledges AYA2008-06202-C03-01.

REFERENCES

Chodas, P. W., & Yeomans, D. K. 1996, in Space Telescope S. I. Symp. Ser. 9, The Collision of Comet Shoemaker-Levy 9 and Jupiter, ed. K. S. Noll, H. A. Weaver, & D. Feldman (Cambridge: Cambridge Univ. Press), 1 Crawford, D. A. 1996, in Space Telescope S. I. Symp. Ser. 9, The Collision of Comet Shoemaker-Levy 9 and Jupiter, ed. K. S. Noll, H. A. Weaver, & D. Feldman (Cambridge: Cambridge Univ. Press), 133

de Pater, I., & Lissauer, J. J. 2010, Planetary Sciences (2nd ed.; Cambridge; Cambridge Univ. Press)

Hammel, H., et al. 1995, Science, 267, 1288

Hammel, H., et al. 2010, ApJ, 715, L150

Harrington, J., & Deming, D. 2001, ApJ, 561, 455

Harrington, J., et al. 2004, in Jupiter, Vol. 159, ed. F. Bagenal, T. Dowling, & W. McKinnon (Cambridge: Cambridge Univ. Press), 159

Jessup, K. L., et al. 2000, Icarus, 146, 19

Kary, D. M., & Dones, L. 1996, Icarus, 121, 207

Kasting, J. F., & Catling, D. 2003, ARA&A, 41, 429

Korycansky, D. G., et al. 2006, ApJ, 646, 642

Levison, H. F., et al. 2000, Icarus, 143, 415

Mac Low, M. 1996, in Space Telescope S. I. Symp. Ser. 9, The Collision of Comet Shoemaker-Levy 9 and Jupiter, ed. K. S. Noll, H. A. Weaver, & D. Feldman (Cambridge: Cambridge Univ. Press), 157

Nakamura, T., & Yoshikawa, M. 1995, Icarus, 116, 113

Orton, G., et al. 2010, Icarus, submitted

Pankine, A. A., & Ingersoll, A. P. 1999, Icarus, 138, 157

Puetter, R. C., & Yahil, A. 1999, in ASP Conf. Ser. 172, Astronomical Data Analysis Software and Systems VIII, ed. D. M. Mehringer, R. L. Lante, & D. A. Roberts (San Francisco, CA: ASP), 307

RegiStax 5 2009, Free Image Processing Software, http://www.astronomie.be/ registax/

Rogers, J. H. 1995, The Giant Planet Jupiter (Cambridge: Cambridge Univ. Press)

Roulston, M. S., & Ahrens, T. J. 1997, Icarus, 126, 138

Schenk, P. M., & Zahnle, K. 2007, Icarus, 192, 135

Schenk, P. M., et al. 2004, in Jupiter, ed. F. Bagenal, T. Dowling, & W. McKinnon (Cambridge: Cambridge Univ. Press), 427

Takata, T., & Ahrens, T. J. 1997, Icarus, 125, 317

Wesley, A. 2009, ninox version 2.71, http://www.acquerra.com.au/astro/software/ ninox/

Zahnle, K. 1996, in Space Telescope S. I. Symp. Ser. 9, The Collision of Comet Shoemaker-Levy 9 and Jupiter, ed. K. S. Noll, H. A. Weaver, & D. Feldman (Cambridge: Cambridge Univ. Press), 183

Zahnle, K., et al. 2003, Icarus, 163, 263

No. 2, 2010 Hammel et al.

HUBBLE IMAGES OF THE 2009 JUPITER IMPACT

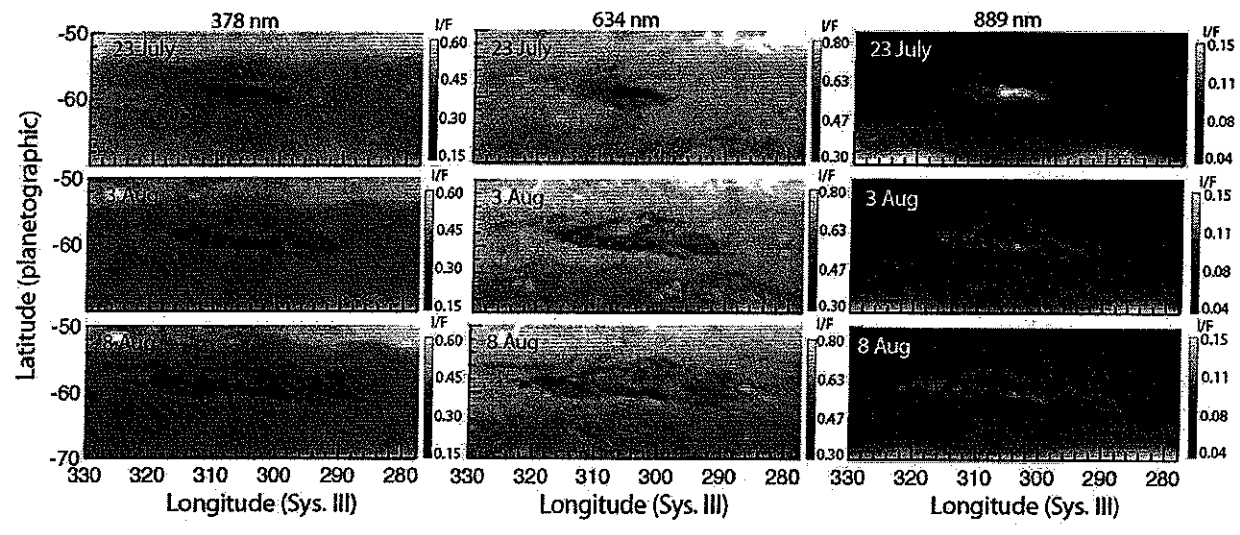


Figure 1. Hubble images showing temporal evolution of the 2009 impact site. (a) Each column in this 3×3 panel shows a different representative wavelength: blue (378 nm), orange (634 nm), and the near infrared (889 nm); full observational log presented in Table 1. The feature appears bright in the 889 nm images because strong methane absorption at that wavelength severely darkens the planet (Figure 2). In the top row (2009 July 23), the characteristic ejecta fan lies to the Jovian northwest (above and to the left of the dark site). In the middle and bottom rows showing August 3 and 8, respectively, Jovian winds acting on the main impact-generated debris clouds disperse the evolving clumps as discussed in the text.

No. 2, 2010 Hammel et al. HUBBLE IMAGES OF THE 2009 JUPITER IMPACT

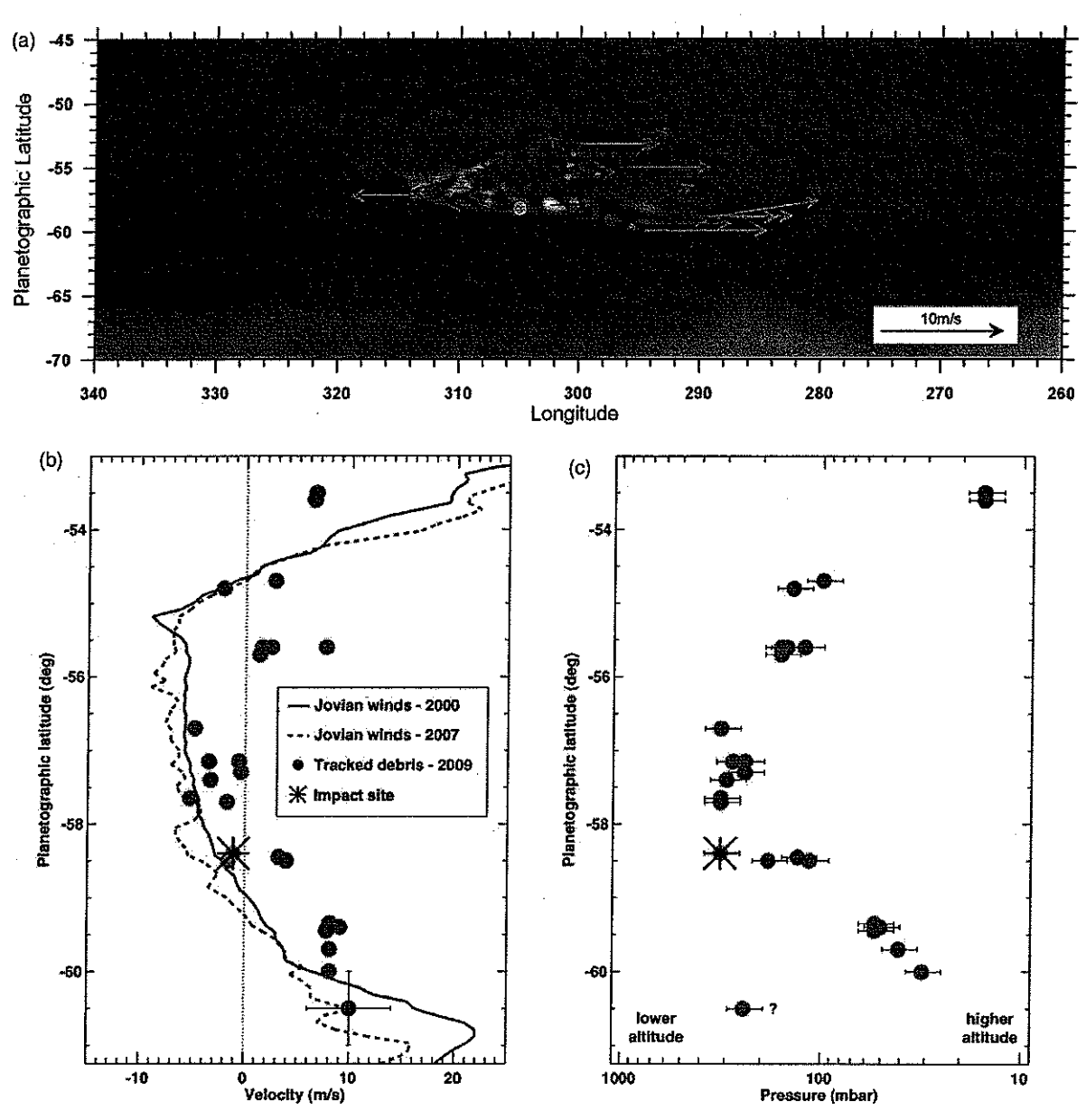


Figure 3. Hubble measurements of the debris motion and altitudes after the 2009 impact. (a) Wind vectors indicate the direction and magnitude of motions measured for specific debris clumps between August 3 (shown here) and 8 (see the bottom row of Figure 1). The initial impact site is marked with a blue circle. The inset shows the length for 10 m s⁻¹; uncertainties, shown on the datum at latitude 60.5°S, are identical for each measurement. (b) Zonal velocities for the debris wind vectors in (a) are plotted as a function of planetographic latitude along with two different measurements of the local zonal winds: the dashed line is unpublished Hubble data from 2007 (A. Sánchez-Lavega et al. 2010a, in preparation); the solid line is Cassini spacecraft data (Porco et al. 2003). The location of the initial impact site is shown with a star. (c) For each debris measurement, we extrapolated the Cassini Jovian zonal wind profile at that planetographic latitude (solid line in (b)) to higher altitudes using the thermal wind equation, and identified the altitude (expressed here as pressure in mbar) where the extrapolated wind velocity matched the observed debris velocity shown in (b). The point at latitude 61°S was the "edge" of a feature rather than a discrete clump, which perhaps accounts for its anomalous altitude.

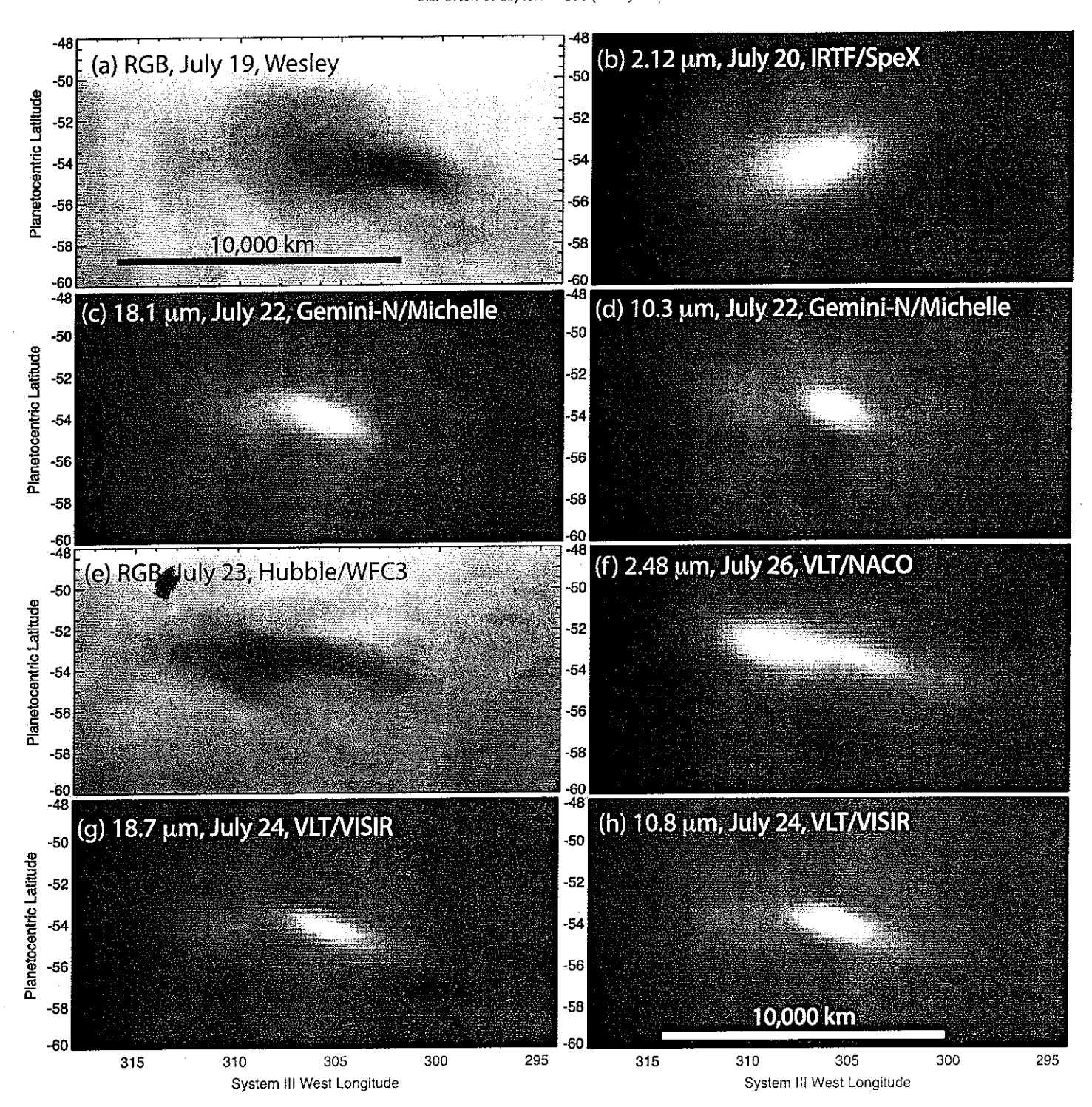


Fig. 2. Cylindrical projections of images of Jupiter centered on the impact site. The images compare observations at different wavelengths and are grouped into two time periods: panels (a)–(d) compare images from July 19–22, and panels (e)–(h) from July 23–26. (a) Color composite of the impact site on the discovery night, July 19 (1), 23°E of the central meridian. (b) 2.12-μm IRTF SpeX (Rayner et al., 2003) guide camera image of the particulate debris field, July 20, distorted by poor seeing, 27°W of the central meridian. (c) False-color 18.1-μm image sensitive to 100-mbar temperatures and (d) 10.3-μm image sensitive to NH₃, both from the Gemini North Michelle instrument (Glasse et al. 1997), July 22, 23°E and 11°E of the central meridian, respectively. (e) Color composite of the impact site from July 23, taken by the Wide-Field Camera 3 on Hubble Space Telescope (Hammel et al., 2010), an average of 25°W of the central meridian. (f) 2.48-μm VLT/NACO (Lenzen et al., 2003; Rousset et al., 2003) image of the particulate debris, July 26, 48°E of the central meridian. (g) False-color 18.7-μm image sensitive to 130-mbar temperatures, 42°E of the central meridian., and (h) 10.8-μm image sensitive to temperatures and NH₃, 35°E of the central meridian; both (g) and (h) are from the Very Large Telescope VISIR instrument (Lagage et al., 2000), July 24. The most intense feature in the center of these frames is the streak, whose center is assumed to be co-located with the impact site in the images closest to the impact date. The less intense and extended feature to its west is the crescent, formed from the re-entry of the impact ejecta (Sánchez-Lavega et al., 2010). The morphology of the various fields are notably changing over the 7 days depicted in this montage, as Jupiter's atmospheric motions redistribute the particulate and warm gaseous material. Although the NASA IRTF images resolve the streak and crescent regions (see Fig. 1), they did not resolve the morphology of the crescent nearly as well as the other images

CUME EXAM # 367 - WITH SUGGESTED SOLUTIONS

This exam is worth 75 points. It is based on the accompanying paper by Sánchez-Lavega et al. (2010), "The impact of a large object on Jupiter in 2009 July" Astrophys. J. Let. 715, L155-L159, plus ancillary materials related to this topic provided from other papers. A grade of 70% or higher is expected to be a passing grade. You may use a calculator, but only for algebraic and trigonometric types of calculations – you may NOT use a calculator to store formulae, constants, etc.

Things You Might Need to Know

 $1 \text{ AU} = 1.496 \times 10^{13} \text{ cm}$ Jupiter's equatorial radius = 71,492 km Jupiter's oblateness = 0.065 Jupiter's rotational period = $9^h55^m27.3^s$ Jupiter's orbital semimajor axis = 5.20 AU $G = 6.674 \times 10^{-8} \text{ dyn cm}^2 \text{ g}^{-2}$

Observations

1. The paper states that the images in methane absorptions show the impact spot to be brighter than its surrounding, suggesting that the material was high in the atmosphere. Explain why a bright debris plume would indicate a high altitude at these wavelengths. (3 points)

Due to the presence of methane in the Jovian atmosphere (at the $\sim 0.2\%$ level), the planet appears dark in strong methane absorption bands because a photon at a CH₄ absorption wavelength gets absorbed by the methane gas before hitting a cloud particle and being reflected or scattered back to the observer. Thus, any feature on Jupiter that is bright in a methane absorption wavelength must be located above the majority of the methane-absorbing gas. [The Great Red Spot is an example of a permanent feature on Jupiter that appears bright in most of the methane absorption bands, indicating that the GRS cloud tops are higher than their surroundings.] NOTE: it is methane gas in Jupiter's atmosphere that is doing the absorbing, not methane clouds. Jupiter is too warm to have clouds made of methane; its uppermost cloud deck is made of ammonia.

2. Panel B in the attached set of images from Figure 2 of Orton *et al.* (2011) shows an image of the plume in an H_2 filter at 2.12 μ m. Yet in astrophysics, we often use CO as a proxy for H_2 in galaxies and the ISM.

a) How is it that we can observe H_2 in Jupiter's atmosphere but not in the ISM? In other words, what makes CO a good proxy for H_2 in the ISM, and why is H_2 not detectable in astrophysical environments but detectable on Jupiter? (3 points)

 H_2 is a homonuclear molecule (made up of multiple atoms of the same element) and therefore does not contain a permanent dipole moment. Thus, in normal (astrophysical) environments, it does not emit or absorb photons because its transitions are forbidden. However, on Jupiter the pressures are high enough that H_2 undergoes collision induced absorption, also known as pressure induced absorption, whereby the molecules collide often enough to induce a temporary dipole moment, which can lead to a transition. In the ISM, pressures are too low for a temporary dipole to be induced for H_2 . CO is used as a tracer for H_2 because it is easily observable in the radio and it is believed to form in similar conditions (cold molecular clouds) as where we would expect the H_2 to be.

b) The H₂ transition at 2.122 μ m is the v=1-0, J=3-1 S(1) line. What does each of those terms mean? (3 points)

The v=1-0 means that the vibrational quantum number is going from 1 to 0, or that the molecule is changing from the v=1 to the v=0 vibrational energy level. The J=3-1 means that the rotational quantum number is going from 3 to 1, or the rotational energy level is changing (ΔJ) by 2. When $\Delta J=\pm 2$, this is known as a quadrupole transition. The S(1) line occurs when J goes from 3-1, while the S(0) line occurs when J goes from 2-0.

c) Contrast your answer in part (b) with a methane absorption band, e.g. at 0.889 μ m. [An image of Jupiter at 0.889 μ m is shown in the attached Figure 1 of Hammel et al. (2010).] What kind of transition(s) give rise to the 0.889 μ m methane absorption band? How is this kind of transition(s) different from a CO line observed at 115 GHz? (4 points)

The methane absorption band at 0.889 μm is a series of absorption lines that are closely spaced, which comprise a set of rotational-vibrational transitions of the CH₄ molecule. In general for molecular spectroscopy, purely rotational transitions are seen at FIR/microwave/radio wavelengths, rovibrational transitions are seen in NIR wavelengths, and electronic transitions are seen at UV wavelengths. A CO line seen at microwave wavelengths is due to a purely rotational transition.

3. The impact was said to be located at a planetocentric latitude of 55.1°. What is the definition of a planetocentric latitude, as opposed to a planetographic latitude, which

is also sometimes used when referring to the giant planets? (2 points)

A planetocentric latitude is measured with respect to the center of the planet, whereas a planetographic latitude is measured with respect to a local normal. See Fig. 1 below. These two forms of latitude only differ from one another for an oblate planet, so they are most often used when referring to coordinates on Jupiter and Saturn. They are related using this equation:

$$tan \theta_g = \left(\frac{R_e}{R_p}\right)^2 tan \theta_c \tag{1}$$

where θ_g and θ_c are the planetographic and planetocentric latitudes, respectively, and R_e and R_p are the equatorial and polar radii, respectively.

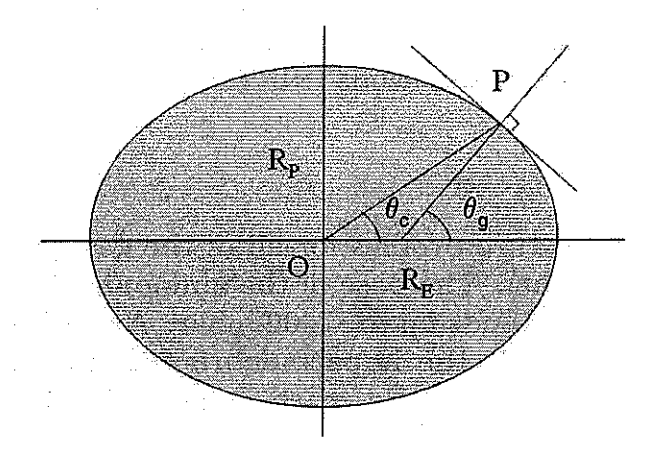


Figure 1: From Sanchez-Lavega, An Introduction to Planetary Atmospheres.

4. From examining the images of the impact shown in Figure 1 of the paper, estimate the seeing that Anthony Wesley must have had from his observing site in Australia in order to obtain those images. Calculate the diffraction limit of his telescope and compare your two numbers, commenting on how the images in Figure 1 could have been obtained. (10 points)

We can start by calculating the diffraction limit of Wesley's telescope, since its diameter is given in the caption of Figure 1:

$$\theta = 1.22 \frac{\lambda}{D} = 1.22 \left[\frac{500 \times 10^{-9} \ m}{0.368 \ m} \right] = 1.66 \times 10^{-6} \ rad = 0.34''$$
 (2)

Jupiter's angular diameter is approximately 40", and the impact site appears to be $\sim 5\%$ the disk diameter, so it is roughly 2" across. The spot is

clearly resolved, so there must be several resolution elements across the 2" spot, thus the seeing must have been sub-arcsecond (probably somewhere around 0.5–1"). This paper does not discuss too many details about the observations (e.g. the exposure time), but one way that amateur Jupiter observers can produce very high quality images with small telescopes is by taking images at VERY high time cadence, with the idea that a small subset of their images are taken in very brief moments of excellent seeing. [This is sometimes referred to as the "lucky imaging" technique.] The post-processing software then goes through and identifies the best images out of the Gigabytes of data acquired in one night.

Giant Planet Atmospheres

5. Draw a Jovian pressure-temperature profile, labeling the axes and the different layers in the atmosphere. Indicate on your P-T profile where the top of Jupiter's uppermost cloud deck lies, as well as the location of the impact debris (HINT: this information can be found in the paper). (10 points)

Figure 2 below shows pressure-temperature profiles for all of the gas giant planets (left) and for Jupiter alone (right). The base of the ammonia cloud deck on Jupiter lies at 700 mbar and it extends up to ~ 400 mbar. According to Figure 3c from Hammel et al. (2010), the impact debris was mostly concentrated around 100 mbar, but some of it did reach pressure levels ~ 10 mbar.

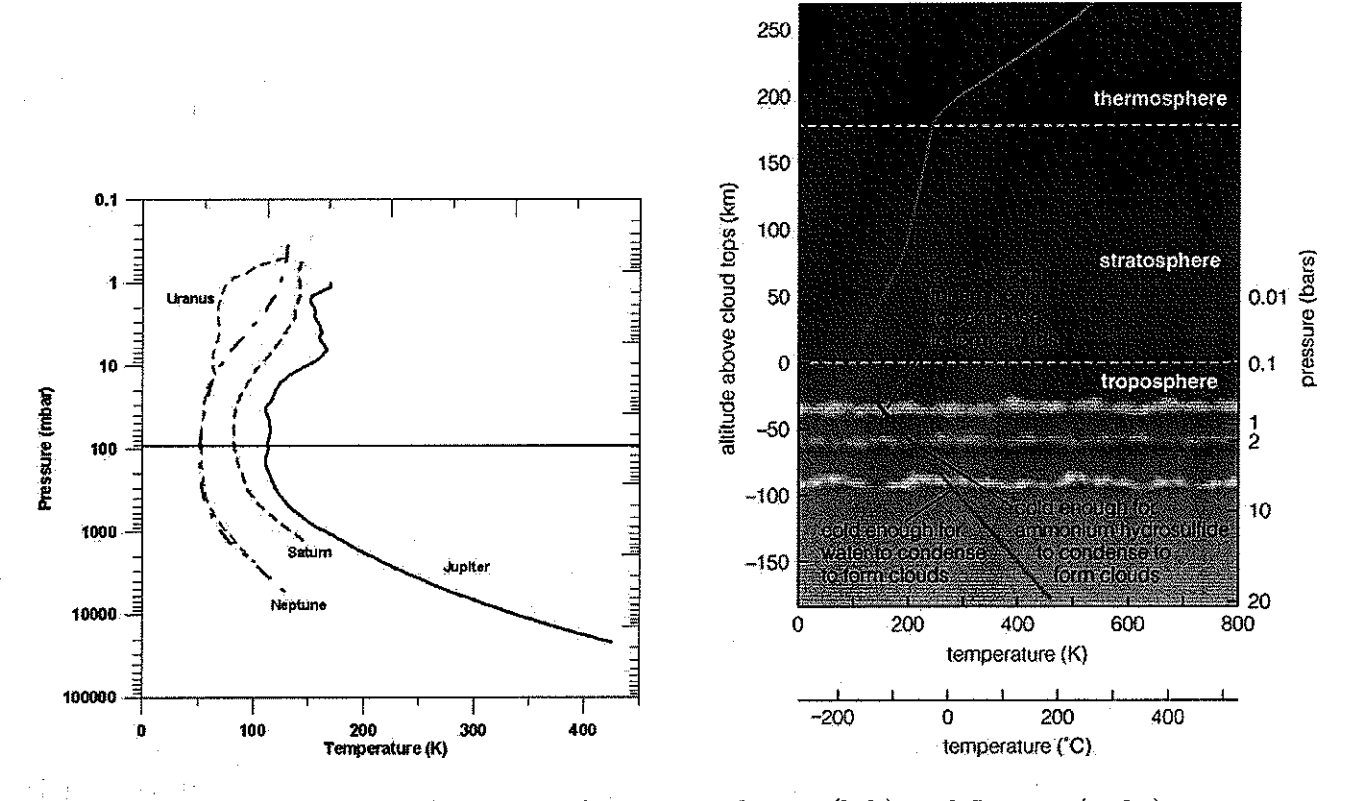


Figure 2: P-T profiles for all four giant planets (left) and Jupiter (right).

6. Figure 3c from Hammel et al. (2010) shows the altitude range of the impact debris. As stated in the figure caption, this information was derived from the data shown in Figure 3b and using the thermal wind equation, which relates the vertical variation of geostrophic winds (winds that are balanced by the Coriolis and pressure gradient forces) to horizontal temperature gradients. Calculate the Rossby number for the winds in the vicinity of the impact site to determine whether in fact the geostrophic approximation holds. (10 points)

The Rossby number can be calculated through a scale analysis of the horizontal momentum equation, and is given by $R_o = U/f_oL$, where U is the zonal (east-west) wind velocity scale, f_o is the Coriolis parameter, and L is the length scale. Plugging in appropriate values: $R_o = (5m/s)/(10^{-4})(3 \times 10^6 m) \approx 0.017$. R_o must be much less than 1 for the geostrophic approximation to hold, so it holds in this case.

Impacts

7. Write a simplified version of Equation 1 for a ballistic trajectory, ignoring the Coriolis force and the sliding of falling material as it enters the atmosphere. Compute the horizontal displacement of material given the best-fit values in the paper for the ejecta

parameters and compare it to the observed size of the impact streak shown in Figure 2c of the paper. Comment on the difference between the two values and how much of an effect you think the inclusion of the Coriolis effect and sliding had on the final result. (10 points)

The geometry of a simple ballistic trajectory is shown in Fig. 3. The hori-

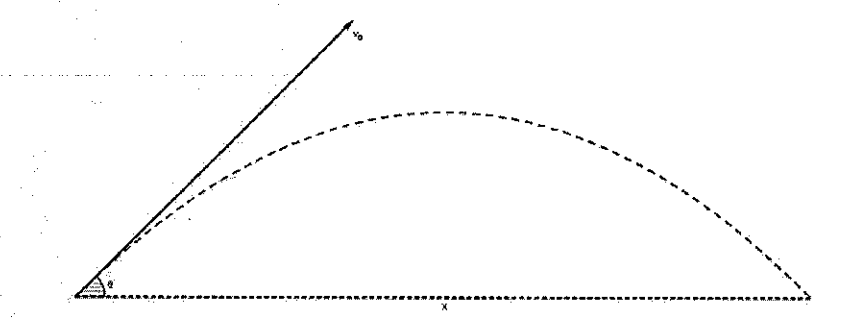


Figure 3: Geometry of a simple ballistic trajectory.

zontal distance as a function of time is given by $x(t) = v cos\theta(t)$. The vertical distance at time t is given by $z(t) = v sin\theta(t) - \frac{1}{2}gt^2$. We are interested in the point when the projectile returns back to the surface (or in the case of Jupiter, the reference pressure level of 100 mbar), where z=0. Solving $0=v sin\theta(t)-\frac{1}{2}gt^2$ for t gives $t=\frac{2v}{g}sin\theta$. Now we can compute what x(t) is for that time t:

$$x(t) = \frac{2v^2}{g} sin\theta cos\theta \tag{3}$$

From the paper, v = 7.6 km/s, g = 25.902 m/s², and $\theta = 20^{\circ}$ (the value quoted in the paper was 70° , but that is as measured from the vertical, not as measured from the horizontal as shown in Fig. 3 above). Solving for x, we get x = 1434 km. According to the paper (in the paragraph after Eq. 3 in the paper), the horizontal streak left by the debris extends for 1600 km, so clearly the inclusion of the Coriolis and sliding effects makes a difference, but is perhaps a second-order effect.

8. Contrast the physics of this impact into Jupiter's atmosphere with the physics of an asteroid impact on the Earth. In your answer, <u>briefly</u> discuss the various stages of impact events and describe the differences between the two scenarios. (10 points)

The different stages of crater formation for solid body impacts are contact and compression, excavation, and modification. The differences for impacts into gas giants are provided below in italics. Contact and Compression: During this stage, the impactor physically makes contact with the target. It travels into the target and penetrates a distance equal to its own diameter in a timescale $\tau = D/v_{imp}$, where D is the impactor diameter and v_{imp} is the impactor velocity. The highest speed ejecta is "squirted" out from the sides as the impactor penetrates into the target, and some of this material will have escape velocity and thus leave the target body. The extreme pressure from the impact produces a shock wave that travels through both the target and the projectile. The projectile gets compressed as the shock wave travels through it; one end doesn't realize that the other end has stopped moving. When the shock wave reaches the rear of the impactor, a rarefaction wave is released; this is what vaporizes the impactor. The total duration of the contact and compression stages is $\sim 1.5\tau$. Even before contact, the ablation of a small body may be more extreme for an impactor into a gas giant because it encounters more and more atmosphere as it descends. This is likely more true for comets than for asteroids. The impactor becomes flattened by aerodynamic forces. The impactor eventually reaches velocities that are greater than the local sound speed (this would also happen when impacting a terrestrial atmosphere); the pressure that builds up in the projectile has no way to "relieve itself" and this eventually results in detonation of the projectile. The surrounding gas also heats up and gets compressed, and violently expands in an explosion that literally punches a hole through the atmosphere, ejecting the heated and compressed gas as well as the vaporized projectile into a high and wide debris plume.

Excavation: During the excavation stage, material is physically removed from the developing crater. It is moved upward and radially outward by a shock wave that propagates hemispherically into the target. The full depth of the crater is reached, and is determined by the strength of the target material, but horizontal expansion continues due to a propagating shock wave. A transient crater is formed by the end of the excavation stage. There is no crater excavation in a gas giant. The projectile gets vaporized and the surrounding atmosphere gets shock heated, resulting in some exotic chemical reactions that do not normally occur in the lower-temperature environments of giant planet atmospheres.

Modification: During the modification stage, the material along the crater walls slumps back down toward the crater center. This results in a final crater that is wider but shallower than the transient crater. By this stage the projectile has been vaporized. The fireball and resulting debris plume rain back down onto the atmosphere, and are visible as differently colored material from the normal clouds (color due to the photochemistry as well as the carbon compounds present in the impactor).

Orbital Mechanics

9. a) The paper discusses the Tisserand parameter, which is a dynamical property that is roughly conserved during an encounter between a planet and a small body; its functional form is as follows:

$$T_J = \frac{a_J}{a} + 2\left[(1 - e^2) \frac{a}{a_J} \right]^{1/2} \cos(i) \tag{4}$$

where a_J is Jupiter's orbital semimajor axis, and a, e, and i are the orbital semimajor axis, eccentricity, and orbital inclination of the small body. The paper mentions Hilda asteroids as a possible source for the impactor that hit Jupiter. The Hildas are a dynamical group of asteroids in a 3:2 mean motion resonance with Jupiter; they have moderate eccentricities and inclinations. Compute T_J for a Hilda asteroid using this information and the above equation. State all of your assumptions. (8 points)

If Hildas are in a 3:2 mean motion resonance with Jupiter, this means that they orbit the Sun three times for every two orbits of Jupiter, i.e. their orbital periods are 2/3 that of Jupiter. From the paper (p. L157), we find that Jupiter's orbital semimajor axis is 5.20 AU. Using the simplified version of Kepler's Third Law, $p^2 = a^3$, we find that Jupiter's orbital period is 11.86 yrs, so the orbital period of the Hildas is ~ 7.9 years. Again using Kepler's Third Law, we find that the orbital semimajor axis of the Hildas is 3.96 AU. Assuming "moderate" values of 0.1 and 20° for the Hildas' orbital eccentricity and inclination, respectively, we can solve for T_J :

$$T_J = \frac{5.20}{3.96} + 2\left[(1 - (0.1)^2) \frac{3.96}{5.20} \right]^{1/2} \cos(20^\circ) = 3.0$$
 (5)

b) Based on the data plotted in Figure 4 of the paper, when must this impactor have been captured by Jupiter in order to definitely have been a Jupiter family comet (as opposed to a Hilda asteroid)? (2 points)

The paper mentions that values of $T_J < 3$ indicate cometary-like orbits while values of $T_J > 3$ indicate asteroidal orbits. According to Figure 4, objects with T_J values < 3 must have been captured by Jupiter very recently, most likely within the last 10 years.